# New Endomorphin Analogues Containing Alicyclic β-Amino Acids: Influence on Bioactive Conformation and Pharmacological Profile

Attila Keresztes,[†] Mária Szűcs,[†] Attila Borics,[†] Katalin E. Kövér,[§] Enikő Forró,[‡] Ferenc Fülöp,[‡] Csaba Tömböly,[†] Antal Péter,[||] Annamária Páhi,[†] Gabriella Fábián,[†] Mariann Murányi,[†] and Géza Tóth*[,†]

*Institute of Biochemistry, Biological Research Center, Hungarian Academy of Sciences, P.O. Box 521, H-6701 Szeged, Hungary, Institute of Pharmaceutical Chemistry, University of Szeged, Eötvös utca 6, H-6720 Szeged, Hungary, Department of Chemistry, University of Debrecen, P.O. Box 21, H-4010 Debrecen, Hungary, Department of Inorganic and Analytical Chemistry, Dóm tér 7, University of Szeged, H-6720 Szeged, Hungary*

*Received March 3, 2008*

Endomorphins were subjected to a number of structural modifications in a search for their bioactive conformations. The alicyclic β-amino acids *cis*-(1*S*,2*R*)ACPC/ACHC, *cis*-(1*R*,2*S*)ACPC/ACHC, *trans*-(1*S*,2*S*)ACPC/ACHC, and *trans*-(1*R*,2*R*)ACPC/ACHC were introduced into endomorphins to examine the conformational effects on the bioactivity. Use of a combination of receptor binding techniques, $^1$H NMR, and molecular modeling allowed the conclusion that Pro$^2$ substitution by these residues causes changes in structure, proteolytic stability, and pharmacological activity. It seems that the size of the alicyclic β-amino acids does not have marked influence on the receptor binding affinities and/or selectivities. Among the new analogues, the *cis*-(1*S*,2*R*)ACPC$^2$ and *cis*-(1*S*,2*R*)ACHC$^2$-containing derivatives displayed the highest binding potencies and efficacies in receptor binding and ligand-stimulated [$^{35}$S]GTPγS functional experiments. Molecular dynamic simulations and $^1$H NMR studies of the *cis*-ACPC/ACHC-containing analogues revealed that many conformations are accessible, though it is most likely that these peptides bind to the μ-opioid receptor in a compact, folded structure rather than extended.

## Introduction

The opioid system, consisting of multiple receptors (μ, δ, and κ) and endogenous peptide ligands (endorphins, enkephalins, dynorphins, and endomorphins), is one of the most extensively studied families among G-protein-coupled receptors. It mediates a wide variety of pharmacological and physiological processes, including pain perception and modulation.[1] Other functions, which involve the respiratory, cardiovascular, gastrointestinal, immune, and neuroendocrine systems, are associated with the development of the undesirable side effects of opioid-based pain management.[2] Two endogenous opioid peptides, endomorphin-1 (Tyr-Pro-Trp-Phe-$NH_2$) and endomorphin-2 (Tyr-Pro-Phe-Phe-$NH_2$), were isolated from the bovine, and subsequently the human CNS.[a3–5] Both amidated tetrapeptides have been shown to be μ-opioid receptor agonists exhibiting very high μ-receptor affinity and selectivity.[3,6,7]

Since their discovery, the endomorphins have aroused considerable interest. No precursor protein or gene encoding their sequences has been identified to date. Although a putative biosynthetic route has been suggested, this is still under investigation.[8] The in vitro metabolic pathway of the endomorphins has been mapped.[9,10] It has been revealed that the aminopeptidases play a key role in the in vitro degradation of endomorphins, the main cleavage sites being the Pro$^2$−Trp$^3$ and Pro$^2$−Phe$^3$ peptide bonds. As concerns proteolytic stability, the endomorphins possess the longest half-lives among the endogenous opioid ligands known so far.[9,10] They belong to the neuropeptide superfamily and are not capable of crossing the blood−brain barrier under physiological conditions due to their low hydrophobicity.[11,12] In animal models, these tetrapeptides have proved to be very effective against inflammatory and neuropathic pain with a reduced cardiorespiratory side effect profile as compared with the prototypical alkaloid ligand morphine.[13–16] This latter fact suggests that the endomorphins are promising lead compounds for the development of novel analgesics. Structural modifications have therefore been considered aiming at improving the pharmacological properties of these relevant drug candidates.

The most frequently applied manipulations in endomorphin engineering involve the incorporation of additional groups, e.g., natural or unnatural amino acids, alterations to the peptide backbone, systematic modification of the pharmacophore groups, and the introduction of conformational constraints.[17,18] Structure−activity studies have demonstrated that Tyr$^1$, Phe$^3$/Trp$^3$, and the amidated C-terminus are essential pharmacophoric elements, required for appropriate binding orientation and μ-receptor recognition.[19–21] Even slight modifications in these aromatic rings, which lead to an appreciable reduction of the conformational freedom, result in changes in affinity and

* To whom correspondence should be addressed. Phone: +36 62 599647. Fax: +36 62 433506. E-mail: geza@brc.hu.

† Institute of Biochemistry, Biological Research Center, Hungarian Academy of Sciences.

‡ Institute of Pharmaceutical Chemistry, University of Szeged.

§ Department of Chemistry, University of Debrecen.

|| Department of Inorganic and Analytical Chemistry, University of Szeged.

[a] Abbreviations: CNS, central nervous system; GTPγS, guanosine-5′-*O*-(3-thio)triphosphate; GDP, guanosine-5′-diphosphate; BSA, bovine serum albumin; EGTA, ethylene glycol-bis(2-aminoethyl ether)-*N*,*N*,*N*,*N*-tetraacetic acid; GITC, 2,3,4,6-tetra-*O*-acetyl-β-glucopyranosyl isothiocyanate; PMSF, phenylmethylsulfonyl fluoride; DMSO, dimethylsulfoxide; DMF, dimethylformamide; TFA, trifluoroacetic acid; DCM, dichloromethane; EtOH, ethanol; Boc, *tert*-butyloxycarbonyl; DAMGO, H-Tyr-D-Ala-Gly-NMe-Phe-Gly-ol; Ile$^{5,6}$-deltorphin-2, H-Tyr-D-Ala-Phe-Glu-Ile-Ile-Gly-$NH_2$; TOCSY, total correlation spectroscopy; ROESY, rotating-frame Overhauser effect spectroscopy; MALDI-TOF, matrix-assisted laser desorption/ionization−time-of-flight; RP-HPLC, reverse-phase high-performance chromatography; TLC, thin-layer chromatography; NOE, nuclear Overhauser effect; MD, molecular dynamics; NMR, nuclear magnetic resonance; rmsd, root-mean-square deviation; VMD, visual molecular dynamics. The abbreviations and definitions used are those recommended by the IUPAC-IUB Commission of Biochemical Nomenclature.

10.1021/jm800223t CCC: $40.75 
Published on Web 06/24/2008

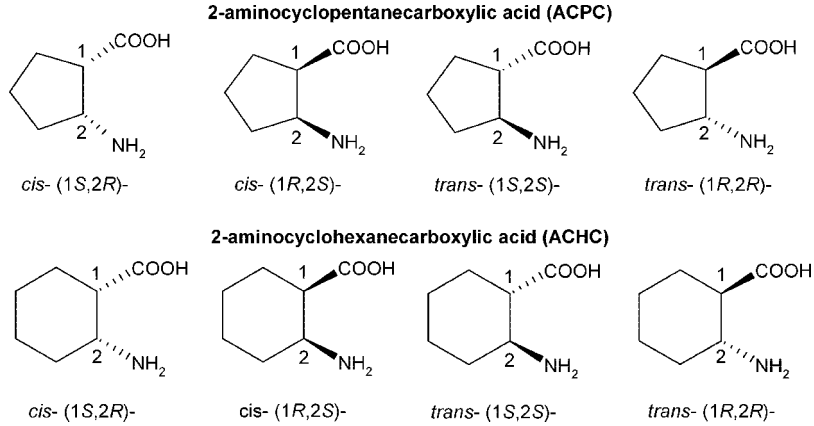


**Figure 1.** Structures of alicyclic β-amino acids incorporated in endomorphin analogues.

selectivity, as observed for the β-methylphenylalanine (βMePhe) and 2,6-dimethyltyrosine (Dmt) containing analogues.[22–24] The effects of substitution of the Phe$^3$ and Phe$^4$ residues of endomorphin-2 with the phenylalanine analogue 2,6-dimethylphenylalanine (Dmp) have also been investigated.[25] L-Dmp substitution in position 3 improves the μ-receptor selectivity and affinity in comparison with the native ligand. Surprisingly the Tyr$^1$ residue, regarded as essential for opioid binding, can be replaced by Dmp with only a slight reduction in μ-receptor affinity.[25]

A large number of data have been reported on the conformational analysis of endomorphins, but the conclusions are rather contradictory as both extended and folded structures have been suggested as the bioactive conformation. The endomorphins exist in *cis* and *trans* conformations with respect to the Tyr$^1$−Pro$^2$ peptide bond.[19] A higher prevalence of the *trans* conformer (*trans*/*cis* ratio = 2:1) has been demonstrated by $^1$H NMR spectroscopic and molecular dynamics studies.[26,27] Aromatic−aromatic interactions between the Tyr$^1$, Trp$^3$, Phe$^3$, and Phe$^4$ side chains have been shown to be important in stabilizing the local conformations of endomorphins.[26] Molecular modeling studies have revealed that the Tyr$^1$−Pro$^2$ interacting pair appears to contribute to the stabilization of the *cis* conformation, while it has been proposed that the Pro$^2$−Phe$^3$, Pro$^2$−Trp$^3$, and Pro$^2$−Phe$^4$ interactions are of less relevance.[26] Substitution of Pro$^2$ by β-(*R*)-Pro or L-homo-Pro residues did not alter or significantly attenuate the affinity of the new derivatives, confirming that Pro$^2$ acts as a stereochemical spacer in these peptides.[17,19,21,28,29]

Considerable knowledge has accumulated concerning the chemistry and chemical utilization of β-amino acids and particularly of 2-aminocyclopentanecarboxylic acid (ACPC) and 2-aminocyclohexanecarboxylic acid (ACHC).[30–33] However, relatively few biochemical and pharmacological data have been published so far on the effects of ACPC or ACHC substitution in opioid peptides.[34–39] Both of these β-amino acids can be regarded as Pro mimetics with a secondary amide. The two chiral centers offer four possible stereoisomers, two configurational *cis*-(*R*,*S* and *S*,*R*) and two configurational *trans*-(*R*,*R* and *S*,*S*) enantiomers (see Figure 1). Substitution of the appropriate α-amino acid residues with these β-amino acids may result in active peptides with altered proteolytic stability and biological activity. ACPC was first incorporated in morphiceptin, a synthetic μ-selective opioid peptide discovered before the endomorphins.[35,36,40] The analogue containing a *cis*-(1*R*,2*S*)-ACPC$^2$ residue was found to adopt a compact structure with a short distance between the Tyr$^1$ and Phe$^3$ residues and to be ∼6 times more active at the μ-receptor and ∼20-times more active at the δ-receptor than morphiceptin. The *cis*-(1*S*,2*R*)-ACPC$^2$ and the corresponding *trans* residue-containing analogues, which adopt more flexible, mainly extended structures, were found to be inactive at both opioid receptors.[36] In other experiments, a relatively large spatial separation of the pharmacophore groups was proposed for the *cis*-(1*S*,2*R*)-ACPC$^2$-containing morphiceptin analogue. Surprisingly, this analogue exhibited the highest potency and selectivity in binding experiments. Yamazaki et al. also found that the configurations of the two chiral centers have a crucial impact on the activity of the analogues and that the *cis*/*trans* isomerization around the Tyr$^1$−Pro$^2$ amide bond is not relevant for biological activity.[35,40]

In the course of the targeted structural modification of endomorphins, we have previously shown that Dmt$^1$ substitution of the Tyr$^1$ residue and/or the incorporation of ACPC/ACHC residues into the position of Pro$^2$ results in analogues with enhanced proteolytic stability.[38] Some of the compounds obtained present dual properties, behaving as a μ-receptor agonist/δ-receptor antagonist. This is noteworthy because mixed μ-agonist/δ-antagonist ligands are believed to have a higher propensity to suppress the development of analgesic tolerance.[41]

We report here on the substitution of Pro$^2$ by all possible stereoisomers of ACPC or ACHC in endomorphin-1 and -2. These peptide analogues were designed to help in elucidating the effects of alicyclic β-amino acid substitution-induced conformational changes on the biological activity of endomorphins. The new peptides were evaluated in radioligand receptor binding experiments in rat brain membrane homogenates, molecular dynamic (MD) simulations, and $^1$H NMR studies. Furthermore, the agonist/antagonist profiles of the endomorphin analogues were assessed in ligand-stimulated [$^{35}$S]GTPγS functional assays.

## Results

**Chemistry.** The incorporation of the Pro mimetics ACPC and ACHC in the position of Pro$^2$ in the endomorphins yielded peptide diastereomers. The ratio of the diastereomeric peptides after the synthesis was nearly 3:1 with respect to the (1*R*,2*S*/1*S*,2*S*)-ACPC$^2$/ACHC$^2$ and (1*S*,2*R*/1*R*,2*R*)-ACPC$^2$/ACHC$^2$-containing analogues. All the new endomorphin analogues were found to be water-soluble. Their analytical properties are listed in Table S1 (see Supporting Information).

The results of the competition experiments led to the selection of four *cis*-ACPC/ACHC-containing endomorphin analogues for degradation studies. It is noteworthy that the β-amino acid substitution prolonged the half-lives of the compounds up to 12 h, in contrast with the short half-lives of endomorphins ($t_{1/2}$

**Table 1.** Inhibitory Constants ($K_i$) of Endomorphin Analogues Containing $\beta$-Amino Acids ACPC or ACHC, Measured in Rat Brain Membrane Preparation

| | | inhibitory constants | | | selectivity | |
|---|---|---|---|---|---|---|
| no. | peptide | $K_i^{\mu}$ (nM)[a] | $K_i^{\mu}$ (nM)[b] | $K_i^{\delta}$ (nM)[c] | $K_i^{\delta}/K_i^{\mu a}$ | $K_i^{\delta}/K_i^{\mu b}$ |
| **1** | endomorphin-1 | 0.74 ± 0.03 | 2.1 ± 0.6 | 1909 ± 233 | 2580 | 909 |
| **2** | [(1*S*,2*R*)ACPC]$^2$endomorphin-1 | 3.6 ± 0.3 | 6.3 ± 1.3 | 1341 ± 122 | 373 | 213 |
| **3** | [(1*R*,2*S*)ACPC]$^2$endomorphin-1 | 275 ± 41 | 196 ± 32 | >10000 | | |
| **4** | [(1*S*,2*S*)ACPC]$^2$endomorphin-1 | 86 ± 8 | 19.9 ± 3.6 | 3075 ± 128 | 36 | 155 |
| **5** | [(1*R*,2*R*)ACPC]$^2$endomorphin-1 | 16 ± 2 | 124 ± 25 | 670 ± 31 | 42 | 5.4 |
| **6** | [(1*S*,2*R*)ACHC]$^2$endomorphin-1 | 1.8 ± 0.5 | 1.5 ± 0.3 | 2763 ± 213 | 1535 | 1842 |
| **7** | [(1*R*,2*S*)ACHC]$^2$endomorphin-1 | 741 ± 61 | 467 ± 103 | >10000 | | |
| **8** | [(1*S*,2*S*)ACHC]$^2$endomorphin-1 | 883 ± 100 | 1120 ± 280 | 9617 ± 6262 | 11 | 8.6 |
| **9** | [(1*R*,2*R*)ACHC]$^2$endomorphin-1 | 1033 ± 81 | 124 ± 22 | >10000 | | |
| **10** | endomorphin-2 | 1.3 ± 0.2 | 1.3 ± 0.2 | 5652 ± 202 | 4348 | 4348 |
| **11** | [(1*S*,2*R*)ACPC]$^2$endomorphin-2 | 2.4 ± 0.1 | 0.72 ± 0.2 | 4798 ± 310 | 1999 | 6664 |
| **12** | [(1*R*,2*S*)ACPC]$^2$endomorphin-2 | 4435 ± 645 | 2049 ± 831 | >10000 | | |
| **13** | [(1*S*,2*S*)ACPC]$^2$endomorphin-2 | 374 ± 61 | 9.9 ± 0.6 | 4228 ± 210 | 11 | 427 |
| **14** | [(1*R*,2*R*)ACPC]$^2$endomorphin-2 | 14 ± 3 | 83 ± 3 | 1411 ± 275 | 100 | 17 |
| **15** | [(1*S*,2*R*)ACHC]$^2$endomorphin-2 | 2.4 ± 0.1 | 0.5 ± 0.1 | 812 ± 18 | 338 | 1624 |
| **16** | [(1*R*,2*S*)ACHC]$^2$endomorphin-2 | 1984 ± 194 | 263 ± 66 | >10000 | | |
| **17** | [(1*S*,2*S*)ACHC]$^2$endomorphin-2 | 166 ± 40 | 144 ± 23 | >10000 | | |
| **18** | [(1*R*,2*R*)ACHC]$^2$endomorphin-2 | 21 ± 1 | 330 ± 65 | 439 ± 41 | 21 | 1.3 |

[a] [$^3$H]DAMGO ($K_d$ = 0.5 nM) and [b] [$^3$H]endomorphin-2 ($K_d$ = 1.0 nM) were used as radioligands for the $\mu$-opioid receptors. [c] [$^3$H]Ile$^{5,6}$deltorphin-2 ($K_d$ = 2.0 nM) was used as radioligand for $\delta$-opioid receptors. $K_i$ values were calculated according to the Cheng−Prusoff equation: $K_i = EC_{50}/(1 + [\text{ligand}]/K_d)$, where the shown $K_d$ values were obtained from isotope saturation experiments. No selectivities were assigned where inhibitory constants proved to be higher than 10000 nM. Data are expressed as means ± SEM, $n \geq 3$.

= 4−5 min), pointing to the enzyme resistance of the new analogues. The detailed experimental procedure has been published elsewhere,[9,10] and the results are summarized in Table S2 (see Supporting Information).

**Biological Evaluation.** Two $\mu$-receptor-selective radioligands, [$^3$H]endomorphin-2 and [$^3$H]DAMGO, were used to test the binding of the new analogues to the $\mu$-opioid receptors. The highly potent and selective $\delta$-receptor agonist [$^3$H]Ile$^{5,6}$deltorphin-2 was applied to measure $\delta$-receptor affinities and selectivities. The inhibitory constants ($K_i$) and selectivities ($K_i^{\delta}/K_i^{\mu}$) of the 16 new analogues are listed in Table 1. The binding values obtained for the parent ligands endomorphin-1 and endomorphin-2 agreed well with literature data.[3,6,7] The new endomorphin derivatives displaced the radiolabeled $\mu$- and $\delta$-receptor specific opioid ligands from a single binding site in a concentration-dependent manner. In general, Pro$^2$ substitution by *cis*-(1*S*,2*R*)-ACPC/ACHC in the endomorphins resulted in analogues with nanomolar inhibitory constants in competing for the tritiated $\mu$-receptor ligands, in accordance with previous reports.[37,38] Compounds **2**, **6**, **11**, and **15** exhibited high affinities, with inhibitory constants from 0.5 up to 6.3 nM. Among these analogues, compounds **6** and **11** containing the *cis*-(1*S*,2*R*)-ACPC$^2$/ACHC$^2$ $\beta$-amino acids displayed the highest $\mu$-receptor selectivities, which were found to be ∼2.0 and ∼1.5 times higher than those of the parent endomorphin-1 and -2, in measurements with [$^3$H]endomorphin-2. These binding data led to the selection of compound **11** for radiolabeling for further detailed binding studies. The synthesis and binding characteristics of [$^3$H][(1*S*,2*R*)ACPC]$^2$endomorphin-2 have been published.[39] Compounds **3**, **7**, **12**, **16**, with *cis*-(1R,2*S*) chiralities, were found to be poor displacers (with micromolar inhibitory constants) of both $\mu$-receptor-specific tritiated ligands. Compound **12** exhibited the lowest potencies ($K_i^{\mu}$ = 4435 and 2049 nM). A surprising outcome of the displacement experiments was that compounds **5**, **14**, and **18**, which contain *trans*-(1*R*,2*R*)-ACPC$^2$ or *trans*-(1*R*,2*R*)-ACHC2, were relatively potent against [$^3$H]DAMGO while they were weaker displacers of [$^3$H]endomorphin-2 binding. As regards these affinity values, there was basically a 1 order of magnitude difference between the *cis*-(1*S*,2*R*)-ACPC$^2$/ACHC$^2$ and *trans*-(1*R*,2*R*)-ACPC$^2$/ACHC$^2$-containing analogues. However, the potency of compound **9** was ∼50−70 times less than that observed for diastereomers **5**, **14**, and **18**, determined against [$^3$H]DAMGO. A profound loss of selectivity was also noted for compounds **5**, **14**, and **18**. Inspection of compounds **4**, **8**, **13**, and **17** revealed that the *trans*-(1*S*,2*S*)-ACPC/ACHC replacements of Pro$^2$ were unfavorable for binding to either opioid receptor. Surprisingly, reduced values ($K_i$ = 19.9 and 9.9 nM) were determined against [$^3$H]endomorphin-2 for compounds **4** and **13**, respectively. In general, the new compounds were found to be poor displacers of the $\delta$-specific [$^3$H]Ile$^{5,6}$deltorphin-2, affording much higher inhibitory constants ($K_i$ = 400 to over 10000 nM) than those observed for the $\mu$-receptor radioligands. The rank order of potency measured by [$^3$H]DAMGO was compounds 1 < 10 < 6 < 15 < 26 < 11 <2 < 14 < 5 < 18 < 4 < 17 < 3 < 13 < 7 < 8 < 9 < 16 < 12, which was not identical to that measured by [$^3$H]endomorphin-2: compounds 15 < 11 < 10 < 6 < 1 < 2 <13 < 4 < 14 < 5 < 26 < 9 < 17 < 3 < 16 < 18 < 7 < 8 < 12.

The selection of compounds for further [$^{35}$S]GTP$\gamma$S functional assay was based upon the binding results ($K_i$ values) of the most potent compounds derived from that of the competition binding experiments. The results of the ligand-stimulated [$^{35}$S]GTP$\gamma$S functional studies are presented in Table 2. Besides the three *cis* diastereomers, compounds **2**, **11**, and **15**, and the parent ligands, four *trans* diastereomer peptides, compounds **4**, **5**, **14**, and **18**, were also chosen. The [$^{35}$S]GTP$\gamma$S stimulations by these ligands were blocked by the universal antagonist naloxone, showing that these ligands act on opioid receptors (data not shown). Potency ($EC_{50}$) and efficacy ($E_{max}$) values were compared with those of the prototype $\mu$-receptor full agonist DAMGO. All of the compounds displayed dose-dependent increases in [$^{35}$S]GTP$\gamma$S binding. The ligand concentrations required to achieve half-maximal stimulation ($EC_{50}$) were 104 nM and 78 nM for the parent endomorphin-1 and endomorphin-2, respectively. Interestingly, both endomorphins exhibited comparable potencies, but lower efficacies ($E_{max}$ = 156% for endomorphin-1 and 148% for endomorphin-2) than those of DAMGO, confirming that the parent endomorphins are partial agonists, as reported earlier.[42,43] Comparison of the efficacies of the *cis*/*trans* analogues and the endomorphins revealed no significant differences, except for compound **15**,

**Table 2.** Summary of [$^{35}$S]GTPγS Functional Assays Carried Out with the Selected ACPC or ACHC-Containing Endomorphins in Rat Brain Membrane Preparations[a]

| no. | peptide | $EC_{50}$ (nM) | $E_{max}$ (%) |
|---|---|---|---|
| **0** | DAMGO | 145 ± 47 | 170 ± 3.3 |
| **1** | endomorphin-1 | 104 ± 29 | 156 ± 4 |
| **2** | [(1*S*,2*R*)ACPC]$^2$endomorphin-1 | 342 ± 81 | 157 ± 5 |
| **4** | [(1*S*,2*S*)ACPC]$^2$endomorphin-1 | 4148 ± 1575 | 129 ± 9 |
| **5** | [(1*R*,2*R*)ACPC]$^2$endomorphin-1 | 396 ± 70 | 137 ± 6 |
| **10** | endomorphin-2 | 78 ± 16 | 148 ± 5 |
| **11** | [(1*S*,2*R*)ACPC]$^2$endomorphin-2 | 353 ± 54 | 163 ± 4 |
| **14** | [(1*R*,2*R*)ACPC]$^2$endomorphin-2 | 2082 ± 773 | 154 ± 5 |
| **15** | [(1*S*,2*R*)ACHC]$^2$endomorphin-2 | 569 ± 114 | 181 ± 9 |
| **18** | [(1*R*,2*R*)ACHC]$^2$endomorphin-2 | 1834 ± 394 | 148 ± 1 |

[a] Dose−response curves of the listed peptides were measured as described in Methods. $EC_{50}$ and $E_{max}$ values were calculated by GraphPad Prism. Data were expressed as % stimulation of the basal activities, i.e. binding in the absence of peptides that was defined as 100%. Means ± SEM, $n \geq 3$, each performed in triplicate.

which exhibited the highest efficacy ($E_{max}$ = 181%), behaving as a full agonist, similarly to DAMGO. In general, the *trans*-ACPC$^2$/ACHC$^2$-containing analogues, compounds **4**, **5**, **14**, and **18** had higher potencies ($EC_{50}$ = 396 up to 4148 nM). Additionally, compounds **4** and **5** displayed the lowest efficacies ($E_{max}$ = 129% and 137%, respectively), suggesting weak partial agonist properties.

**Structural Studies.** Compounds **2**, **3**, **11**, and **12** were selected for structural studies in view of their biological properties. These peptides displayed different μ-opioid receptor affinity and selectivity depending on the configuration of the ACPC$^2$ residue. Our aim was to identify how the stereochemistry of ACPC affects backbone conformation and therefore bioactivity. Short peptides containing a β-amino acid demonstrate different secondary structures from those of all α-amino acid-containing peptides. Their backbone is only one carbon atom longer, but their conformation cannot be described by the classical secondary structural definitions alone. Accordingly, new secondary structural elements had to be defined for their precise description.

The NMR studies of compounds **2**, **3**, **11**, and **12** were carried out in DMSO-$d_6$. DMSO-$d_6$ is a widely used solvent in NMR studies of peptides, including enkephalins, because its biophysical properties are comparable with those of extracellular aqueous solutions. Several other solvents, solvent mixtures,[44] were proposed previously to better approximate the physical properties of such environment, but the moderate structure destabilizing effect[45] of DMSO makes it more suitable for the detection of solvent independent, intrinsic structural properties that are most likely to be in relation with bioactivity. The $^1$H chemical shifts were assigned following the standard protocol of Wüthrich,[46] utilizing 2D TOCSY and ROESY experiments.[47] $^1$H NMR parameters such as the chemical shifts (δ) of amide and aliphatic protons, and intraresidue geminal ($^2J$) and vicinal ($^3J$) coupling constants are reported in Tables S3 and S4 (see Supporting Information).

The $^1$H NMR spectrum of each peptide contained only one set of signals, indicating the presence of one predominant isomer. The ROESY spectra yielded no experimental evidence of a *cis*-peptide bond in the studied analogues. In the structure calculations, therefore, the peptide bond was constrained to the *trans* configuration. The *cis* configuration of ACPC$^2$ in peptides **2**, **3**, **11**, and **12** was confirmed by the strong ROESY crosspeaks observed between $H_α$ and $H_β$ for each analogue. The assignment of the two possible *cis* isomers ((1*R*,2*S*)-ACPC$^2$ and (1*S*,2*R*)-ACPC$^2$) was confirmed by using NOEs and vicinal proton−proton coupling constants ($^3J_{NH-CH}$). For the *cis*-(1*R*,2*S*)-ACPC$^2$ analogues, the $^3J_{NH-CH}$ was 8.7 Hz, while for the *cis*-(1*S*,2*R*)-ACPC$^2$ isomer, 8.1 Hz was observed. The coupling constants $^3J_{NH}$ and $^3J_{Hαβ}$ in Tables S3 and S4 (see Supporting Information) are related to the backbone conformation and the mean orientation of the side chain groups. The population percentages of the three staggered rotamers around the $C_α-C_β$ bond were calculated for the aromatic side chain groups (Tyr, Trp, and Phe) by utilizing the Pachler parametrization of the Karplus equation.[48,49] The *gauche* (−) and *trans* rotamers could be assigned via the stereospecific assignment of the $H_β$s obtained from the 2D ROESY experiments. The calculated rotamer populations are given in Table S5 (see Supporting Information). The distance restraints obtained from the ROESY spectra were included throughout the structure refinement process. To avoid biasing the structures, only unambiguous manually assigned ROESY crosspeaks were used in the calculations.

The conformational ensemble generated by using distance geometry and NOE-derived interproton distances consisted of three markedly different conformational families for each peptide. Besides random/extended structures, bent structures were found, which were similar to the β-turn structures of all α-amino acid-containing peptides. Furthermore, $C_8$-turns around the ACPC$^2$ residue, similar to γ-turns, were identified. Following the classification rules of γ-turns, classic $C_8$-turns were found in the *cis*-(1*R*,2*S*)-ACPC$^2$-containing analogues and inverse $C_8$-turns in the *cis*-(1*S*,2*R*)-ACPC$^2$-containing peptides.

MD simulations of all peptides were performed, starting from extended, bent, and $C_8$-turn structures with the NOE interproton distances incorporated as restraints. Unrestrained MD simulations were also carried out to confirm that no possible conformational state remained undetected due to the relatively slow sampling time scale of NMR. The results of MD simulations and trajectory analyses are presented in Tables 3 and 4 and Figure 2. Side chain rotamer populations (Table 3) were determined in comparison with those derived from the NMR data. While the unrestrained simulations gave acceptable results in some cases, restrained MD failed to reproduce the experimental data. The distances between the three putative pharmacophore groups were measured and evaluated according to the literature data.[40] The fraction of the MD-derived structural ensemble, in which all three distances are in the correct range is included in Table 4. The results show that each peptide is capable of adopting a structure in which the pharmacophore groups are in the suggested arrangement. However, this was not confirmed by the results of restrained MD, and no correlation was observed with the biological data.

Because these peptides may adopt unusual secondary structures, classic secondary structure-recognizing algorithms, such as DSSP[50] or STRIDE,[51] may give false results. The secondary structural properties of these compounds were therefore studied by measurement of the $C_α(1)-C_α(4)$ distance and the virtual dihedral angle defined by $C(1)-C_α(2)-C_α(3)-N(4)$. The results showed that peptides incorporating *cis*-(1*S*,2*R*)-ACPC$^2$ are more prone to adopt a bent structure than those having *cis*-(1*R*,2*S*)-ACPC in position 2. This correlates well with the biological data, where *cis*-(1*S*,2*R*)-ACPC$^2$-containing analogues were found to be more potent than those containing *cis*-(1*R*,2*S*)-ACPC$^2$. The secondary structure was further studied by clustering and identification of the specific intramolecular H-bonds. As expected, more possible conformers were found by clustering when no distance restraints were applied. Six specific intramolecular H-bonds were searched for along the trajectories, and their occurrence was expressed as a percentage of the total structural ensemble generated by MD. These H-bonds stabilize

**Table 3.** Side Chain Rotamer Populations of Compounds **2**, **3**, **11**, and **12** Determined by NMR Studies and MD Simulations

| | | ACPC2-EM-1 | | | | ACPC2-EM2 | | | |
|---|---|---|---|---|---|---|---|---|---|
| | | 1*R*,2*S* (**3**) | | 1 *S*, 2*R* (**2**) | | 1 *R*,2*S* (**12**) | | 1 *S*,2*R* (**11**) | |
| | | Unrest. MD | Rest. MD[a] | Unrest. MD | Rest. MD[a] | Unrest. MD | Rest. MD[a] | Unrest. MD | Rest. MD[a] |
| Tyr[1] | g+ | 7.2 | 0.0 (30.4) | 17.6 | 33.8 (34.3) | 13.5 | 0.0 (33.8) | 2.8 | 0.6 (34.3) |
| | g− | 22.6 | 100.0 (66.2) | 31.6 | 66.2 (35.3) | 27.3 | 100.0 (66.2) | 30.6 | 99.4 (35.3) |
| | t | 70.2 | 0.0 (3.4) | 50.8 | 0.0 (30.4) | 59.2 | 0.0 (0.0) | 66.6 | 0.0 (30.4) |
| Trp[3]/Phe[3] | g+ | 48.8 | 0.0 (41.1) | 46.3 | 0.0 (30.4) | 18.8 | 0.0 (30.4) | 19.7 | 14.9 (23.6) |
| | g− | 17.1 | 0.0 (16.9) | 24.9 | 99.0 (63.3) | 8.4 | 0.0 (37.2) | 7.8 | 0.0 (73.0) |
| | t | 34.1 | 100.0 (42.0) | 28.8 | 1.0 (6.3) | 72.8 | 100.0 (32.4) | 72.5 | 85.1 (3.4) |
| Phe[4] | g+ | 18.9 | 0.0 (43.9) | 13.7 | 2.1 (41.0) | 6.8 | 0.0 (35.3) | 4.5 | 0.0 (35.2) |
| | g− | 14 | 7.2 (44.0) | 22.3 | 64.6 (44.0) | 12.8 | 0.6 (47.8) | 9.9 | 0.0 (46.9) |
| | t | 67.1 | 92.8 (12.1) | 64 | 33.3 (15.0) | 80.4 | 99.4 (16.9) | 85.6 | 100.0 (17.9) |

[a] Populations calculated directly from NMR data are shown in parentheses.

**Table 4.** Specific Structural Properties of Compounds **2**, **3**, **11**, and **12** as Obtained from MD Simulations

| | | | ACPC[2]-EM-1 | | | | ACPC[2]-EM-2 | | | |
|---|---|---|---|---|---|---|---|---|---|---|
| | | | 1*R*,2*S* (**3**) | | 1*S*,2*R* (**2**) | | 1*R*,2*S* (**12**) | | 1*S*,2*R* (**11**) | |
| | | | Unrest. MD | Rest. MD | Unrest. MD | Rest. MD | Unrest. MD | Rest. MD | Unrest. MD | Rest. MD |
| occurrence of specific intramolecular H-bonds[a]/% | Tyr[1]-CO—HN-Trp[3]/Phe[3] | (C, D) | 2.0 | >0.1 | 7.2 | 0.0 | 0.0 | 0.0 | 11.6 | >0.1 |
| | ACPC[2]—CO-HN-Phe[4] | (E, F) | 7.8 | 91.4 | 8.5 | 4.8 | 4.2 | 0.5 | 5.2 | 8.4 |
| | Tyr[1]-CO—HN-Phe[4] | (A) | 1.7 | 0.0 | 13.4 | 0.0 | 0.2 | 0.0 | 4.0 | 0.0 |
| | Tyr[1]-NH—OC-Trp[3]/Phe[3] | (K) | 9.4 | 0.0 | 0.0 | 0.0 | 0.8 | 0.0 | 1.3 | 2.6 |
| | ACPC[2]—NH—OC-Trp[3]/Phe[3] | (B) | 21.1 | 0.0 | 29.1 | 0.1 | 5.4 | 0.0 | 26.2 | 0.8 |
| | ACPC[2]—CO—$H_2$N-CO-Phe[4] | (J) | 32.2 | 12.8 | 5.3 | 0.0 | 19.3 | 0.3 | 3.9 | 0.0 |
| occurrence of bent structure[b]/% | | | 29.8 | 91.8 | 70.0 | 66.4 | 16.9 | 24.0 | 77.0 | 87.6 |
| pharmacophoric distances[c]/% | | | 2.1 | 0.0 | 1.0 | >0.1 | 2.8 | 0.0 | 4.9 | >0.1 |
| no. of clusters | | | 39.0 | 10.0 | 117.0 | 12.0 | 99.0 | 13.0 | 92.0 | 9.0 |
| possible conformations[d] | | | A, B, C, D, F, G, H, J, L | D, F, G, H, J, L | A, B, C, D, F, H, J, K, L | A, K, L | A, B, E, F, J, K, L | F, G, H, J, L | A, B, C, E, F, G, I, J, K, L | B, C, F, G, K, L |

[a] Stabilized conformations according to the lettering in Figure 2 are shown in parentheses. [b] Bent structure was assigned through analysis of the N(1)−$C_\alpha$(2)−$C_\alpha$(3)−C(4) virtual dihedral angle and the distance between the terminal $C_\alpha$ atoms. [c] Occurrence of structures in which all pharmacophoric distances are in the correct range. [d] See Figure 2 for the explanation of the lettering.

the following secondary structural elements: a $C_8$-turn around ACPC[2] (Figure 2C−D), a $\gamma$-turn around Trp[3]/Phe[3] (Figure 2E−F), a $C_9$-turn around ACPC[2]-Trp[3]/Phe[3] (Figure 2B), a $C_{11}$-turn around ACPC[2]-Trp[3]/Phe[3] (Figure 2A), C-terminal $\beta$-turn around Trp[3]/Phe[3]−Phe[4] (Figure 2J), and a $C_{12}$ ring formed by a H-bond between the N-terminal free amine and the C═O group of Trp[3]/Phe[3] (Figure 2K). Besides extended/random structures, two further distinct structural families were found after clustering: $C_7$ (Figure 2H−I) and $C_{10}$-turn (Figure 2G) structures. These were analogous to the $\gamma$-turn and $\beta$-turn structures, respectively, but, instead of specific CO and NH groups facing each other to form stabilizing H-bonds as in regular $\gamma$- and $\beta$-turns, here two NH groups are in such proximity. However, NHN H-bonds can not be formed not only because of the unfavorable position of these groups but because of the delocalization of the electrons of the amide N.

## Discussion

Definite structural characteristics of the bioactivity of endomorphins have not yet been identified. Apart from the biochemical significance of the well-defined pharmacophore groups, the published fundamental role of Pro[2] as a stereochemical spacer[17,26] has been confirmed by our results. The extensively examined *cis*−*trans* isomerization around the Tyr[1]−Pro[2] peptide backbone permits the endomorphins to adopt many accessible conformations.[19] In this study, conformational constrains were introduced into the peptide sequence to control this dynamic process. These modifications diminished the *cis*/*trans* isomerization of the amide bond between Tyr[1] and ACPC[2]/ACHC[2]. The incorporation of racemic alicyclic $\beta$-amino acids, and particularly *cis*/*trans*-ACPC and *cis*/*trans*-ACHC, yielded a series of peptide analogues with altered proteolytic stabilities and pharmacological activities. The effects of the configuration of the alicyclic $\beta$-amino acids and the *cis*/*trans* isomerization on the biological activity were studied on 16 diastereomer peptides.

In our study, a trend of adverse potencies was measured for *cis*-ACPC[2]/ACHC[2]-containing analogues of endomorphins as compared with that suggested by Mierke et al. for the *cis*-ACPC-containing morphiceptin analogues.[36] Compounds with *cis*-(1*S*,2*R*)-ACPC[2]/ACHC[2] residues were assessed to be as potent as the native ligands and more potent than those with *cis*-

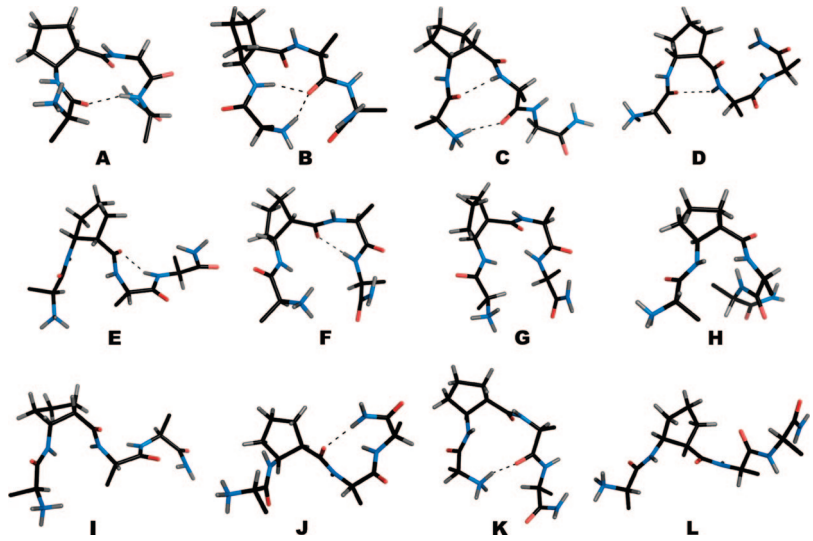


**Figure 2.** Possible conformation of compounds **2**, **3**, **11**, and **12** (aromatic side chains are omitted for clarity). (A) $C_{11}$-turn, (B) $C_9$-turn, (C) "classic" $C_8$-turn, (D) "inverse" $C_8$-turn, (E) classic $\gamma$-turn, (F) inverse $\gamma$-turn, (G) $C_{10}$-turn, (H) "classic" $C_7$-turn, (I) "inverse" $C_7$-turn, (J) C-terminal $\beta$-turn, (K) N-terminal $C_{12}$-loop, (L) random/extended.

(1*R*,2*S*)-ACPC$^2$/ACHC$^2$ residues. Potent diastereomers were additionally found among the *trans*-ACPC$^2$/ACHC$^2$-containing endomorphin analogues, suggesting that the *cis*-(1*R*,2*R*)-ACPC$^2$/ACHC$^2$-containing analogues adopt conformations similar to those of the *cis*-(1*S*,2*R*)-ACPC$^2$/ACHC$^2$-containing ones. This is noteworthy because the *trans*-ACPC-containing analogues of morphiceptin were shown in earlier binding experiments to be inactive.[35,36] Our results confirmed that the chirality and spatial orientation may be very important features determining the biological activity of a peptide. Furthermore, our data suggest that the Phe$^3$ or Trp$^3$ residues and the size of the alicyclic $\beta$-amino acids do not have a marked influence on the receptor binding. The findings of competition experiments indicated that alicyclic $\beta$-amino acid substitution of Pro$^2$ in the endomorphins led to a considerable reduction of the $\mu$- vs $\delta$-receptor selectivity.

The agonist and antagonist properties were determined by using the [$^{35}$S]GTP$\gamma$S binding assay, which reflects the interactions between the ligand-activated opioid receptors and the regulatory $G_i$/$G_o$-proteins. The results of [$^{35}$S]GTP$\gamma$S experiments clearly demonstrated that alicyclic $\beta$-amino acid substitutions do not exert pronounced effects on the agonist/antagonist properties. The examined analogues mostly retained partial agonist profiles similar to those of the endomorphins. The competition and [$^{35}$S]GTP$\gamma$S binding experiments indicate that the receptor affinity and selectivity are governed by diverse structural aspects after the introduction of alicyclic $\beta$-amino acids. It should be noted that compounds **4**, **5**, **9**, **13**, **14**, **16**, and **18** exhibited significantly different inhibitory constants when measured against [$^3$H]DAMGO or [$^3$H]endomorphin-2, while the parent ligands, compounds **1** and **10**, displayed comparable values. One possible explanation is that although both DAMGO and endomorphin-2 bind with high affinity and selectivity to the $\mu$-opioid receptor, they may bind to different regions and induce different affinity states of the protein. In accordance with this explanation, it was shown that while DAMGO discriminates between $\mu$- and $\delta$-opioid receptors by recognizing the difference in only one amino acid residue, endomorphin-1 differentiates between them based on differences widely distributed through the receptor structure.[52,53] It has been raised that DAMGO and endomorphin-2 may bind to different subtypes of the $\mu$-opioid receptor,[21,54–56] although the existence of such subtypes is still controversial. Finally, homo- and hetero-oligomerization of the opioid receptors have been documented in numerous reports and are of particular interest because these processes may entail profound changes in ligand binding and/or signaling profile and also analgesia.[57–62] Thereby, we found it advantageous to characterize the new analogues with two distinct radioligands, even if no clear-cut conclusion about their preference for the *cis*- or *trans*-isomers can be made at present.

The inconsistencies between the results of unrestrained and restrained MD simulations suggest that these peptides may exist in more conformational states than were detected by NMR. It is well established that, due to the relatively slow NMR data acquisition response time, time-averaged parameters are obtained when fast conformational exchange occurs.[63] Furthermore, it has been found that side chain rotamer populations estimated from the coupling constants $^3J_{H\alpha-H\beta}$ cannot be reproduced by restrained MD. However, this is most probably a limitation of the restrained MD approach and the uncertainty in the parametrization of the relevant Pachler equation proposed for the $^3J_{H\alpha-H\beta}$ coupling. Restrained simulated annealing studies may be a more sensible choice for the evaluation of these structural parameters.

Distances between pharmacophore groups, earlier proposed to be a requirement for biological activity, were measured in a mainly unordered structures of morphiceptin and morphiceptin analogues possessing a *cis* Tyr$^1$−Pro$^2$ peptide bond.[35,36] However, different backbone structures have been hypothesized to be responsible for $\mu$-opioid receptor affinity and selectivity in numerous other studies.[17,26] These distances may therefore not be as important as thought previously. Nevertheless, our studies indicate that compounds **2**, **3**, **11**, and **12** are able to adopt a structure in which the pharmacophores are in the correct spatial arrangement according to the proposal of Yamazaki et al.[35,40]

In contrast with earlier observations on ACPC-containing morphiceptin analogues,[35,40] it was found that endomorphin analogues, in which Pro$^2$ is substituted by cis-(1*S*,2*R*)-ACPC$^2$ adopt a bent structure more readily than in the case of the *cis*-(1*R*,2*S*)-ACPC-containing analogues. These analogues displayed significantly higher affinities for the $\mu$-opioid receptor, suggesting that a higher tendency to form a bend or a turn may be important for receptor binding. This is in accordance with previous results, when potent opioid analogues with constrained turn structure were obtained.[64] Various bend, turn, and extended

structures were identified as possible conformations of the analogues studied here by clustering and the analysis of specific intramolecular H-bonds. This additionally agrees with earlier findings on endomorphins,[65,66] although several unique structural elements were in consequence of the elongation of the peptide backbone by incorporation of a $\beta$-amino acid. As concerns the biological data on these analogues, it seems plausible that this elongation does not significantly affect the folding of these peptides or the orientation of the pharmacophoric elements, which further confirms the role of $Pro^2$ as a stereochemical spacer. Most of these special secondary structural elements were found to be stabilized through intramolecular H-bonds. The exceptions were the $C_7$-turn and $C_{10}$-turn structures, where such H-bonds cannot be formed. These structures are most likely stabilized through aromatic−aromatic or aromatic−CH interactions. Such interactions were not analyzed in this study, but there have been a number of reports regarding their importance in the stabilization of local structures in opioid and other peptides.[67,68]

## Conclusions

The alicyclic $\beta$-amino acids *cis*-(1*S*,2*R*)-$ACPC^2$/$ACHC^2$, *cis*-(1*R*,2*S*)-$ACPC^2$/$ACHC^2$, *trans*-(1*S*,2*S*)-$ACPC^2$/$ACHC^2$, and *trans*-(1*R*,2*R*)-$ACPC^2$/$ACHC^2$ were introduced into endomorphins in order to examine the effects of the conformations on the bioactivity. From a combination of different receptor binding techniques, $^1$H NMR studies, and molecular modeling, it was concluded that $Pro^2$ replacement by these residues leads mostly to proteolytically stable peptide analogues, with the retention of pharmacological activity, in accordance with earlier observations. In general, the analogues containing *cis*-(1*S*,2*R*)-$ACPC^2$/$ACHC^2$ exhibited the highest $\mu$-opioid receptor affinities, which were comparable with those of the parent endomorphins. The synthesized compounds displayed diverse in vitro potencies as measured in competition and GTP$\gamma$S experiments. The importance of the configurations of the alicyclic $\beta$-amino acids was confirmed by molecular modeling studies. Various possible conformations were proposed for compounds **2**, **3**, **11**, and **12**, and the bioactive structure is most probably to be found among them. The conformational studies were performed on isolated molecules in aqueous media, and therefore the most populated conformational family does not necessarily correspond to the bioactive structure, but a higher propensity of various turn structures was observed for the analogues with higher receptor affinities. This suggests that these peptides might bind to the $\mu$-opioid receptor in a compact, folded structure rather than an extended one.

## Experimental Section

**General Methods.** Natural amino acids were purchased from Reanal (Budapest); alicyclic $\beta$-amino acids were synthetized in our laboratory. The lipolase (lipase B of the *C. antarctica* organism) applied for the enantioselective ring opening and amino ester hydrolysis was purchased from Sigma-Aldrich Kft (Budapest, Hungary). The Boc-protection of amino acids was carried out locally, and 4-methylbenzhydrylamine resin (MBHA) was purchased from Bachem Feinchemicalen AG (Bubendorf, Switzerland). TLC was performed on chiral TLC plates (Macherey Nagel, Dürer, Germany) or on silica gel 60 $F_{254}$ from Merck (Darmstadt, Germany), using the following solvent systems: (A) 1-butanol/acetic acid/water (4:1:1:), (B) acetonitrile/methanol/water (4:1:1). Spots were visualized under UV light or with ninhydrin reagent. HPLC separation and analysis of all compounds were performed with a complete HPLC system consisting of an L-7100 pump (Merck KGaA, Darmstadt, Germany), a SIL-6B autosampler (Shimadzu Co., Kyoto, Japan), a Shimadzu SCL-6B system controller, and a Merck L-7400 UV−vis detector, operating at 215 nm with a Hitachi D-7000 HPLC system manager. Samples were analyzed on Vydac 218TP1010 (250 mm × 10 mm, 12 $\mu$m) and Vydac 218TP54 (250 mm × 4.6 mm, 5 $\mu$m) $C_{18}$ reverse-phase columns at a flow rate of 4 mL/min or 1 mL/min, at room temperature. The mobile phase was composed of 0.1% (v/v) TFA in water and 0.08% (v/v) TFA in acetonitrile (Merck), and gradient elution was carried out with 15% up to 40% organic modifier. The eluents were directly sonicated before use. Injected samples were filtered through a 0.45 $\mu$m Whatman PTFE syringe filter (Clifton, NJ). The purities of the inactive peptides were confirmed by mass spectrometry using a Reflex III MALDI-TOF instrument (Bruker Bremen, Germany) in the positive reflectron mode.

Tritiated radioligands, such as [$^3$H]DAMGO (1.6 TBq/mmol, 43 Ci/mmol), [$^3$H]Ile-$^{5,6}$deltorphin-2 (1.5 TBq/mmol, 39 Ci/mmol), and [$^3$H]endomorphin-2 (1.9 TBq/mmol, 51 Ci/mmol) were prepared on site from the appropriate halogenated or unsaturated peptide derivatives by tritium dehalogenation or saturation, except for the stabilized [$^{35}$S]GTP$\gamma$S (42 TBq/mmol, 1133 Ci/mmol), which was purchased from Amersham (GE Healthcare, United Kingdom). Incubation mixtures were filtered by a M24R Brandel cell harvester (Gaithersburg, MD). Filter-bound radioactivities were detected and measured in a TRI-CARB 2100TR liquid scintillation analyzer (Packard), using a toluene-based cocktail containing 2,5-diphenyloxazole (PPO, Reanal) and 1,4-bis(4-methyl-5-phenyl-2-oxazolyl)-benzene (POPOP, Reanal). All NMR data were acquired on a Bruker DRX-500 spectrometer and processed with the Bruker XWINNMR software. Biological data were analyzed by using GraphPad Prism software (version 4.0, San Diego, CA).

**Synthesis of the Saturated 2-Aminocyclopentanecarboxylic (ACPC) and 2-Aminocyclohexanecarboxylic (ACHC) Acids.** The detailed procedures for the synthesis of the alicyclic $\beta$-amino acids have been published elsewhere.[69] Briefly, racemic *cis*-ACPC and *cis*-ACHC were prepared from the corresponding cycloalkene by chlorosulfonyl isocyanate addition, followed by ring opening with hydrochloric acid. The *trans* counterparts were prepared from the corresponding 1,2-dicarboxylic anhydrides after amidation, followed by Hofmann degradation with hypobromite.[30] The enantiomers of *cis*-ACPC and *cis*-ACHC were prepared through lipolase-catalyzed enantioselective ring cleavage of the corresponding $\beta$-lactams,[70] while the enantiomers *trans*-ACPC and *trans*-ACHC were obtained through enzymatic hydrolysis of the alicyclic $\beta$-amino esters.[71] The chemical structures of the alicyclic $\beta$-amino acids are shown in Figure 1.

**Solid-Phase Peptide Synthesis and Peptide Purification.** The peptide analogues were synthesized by using *N*-α-*t*-Boc-protected amino acids and MBHA resin to obtain C-terminal amides. All the amino acids were protected manually with di-*tert*-butyl-dicarbonate (Fluka). *cis*-(1*S*,2*R*/1*R*,2*S*)-ACPC or *cis*-(1*S*,2*R*/1*R*,2*S*)-ACHC and *trans*-(1*S*,2*S*/1*R*,2*R*)-ACPC or *trans*-(1*S*,2*S*/1*R*,2*R*)-ACHC were incorporated into the peptides in racemic form. Coupling reagents were *N*-hydroxybenzotriazole (Novabiochem) and *N*,*N*-dicyclohexylcarbodiimide (Merck) for peptide elongation. Coupling was monitored by the Kaiser test.[72] The protecting groups were removed by washing the resin with a combination of 50% TFA, 48% DCM containing 2% anisole (Merck). The resin was washed repeatedly with EtOH (Molar) and DCM between two coupling steps. Neutralization was performed with 20% diisopropylethylamine (Merck) in DCM. The peptides were cleaved with anhydrous liquid HF (5 mL/g resin, 1 h, 0 °C) in the presence of anisol (1 mL/g resin). Dry, peroxy-free diethyl ether (Reanal) was used to precipitate the cleaved peptides. After precipitation the peptides were filtered off, dissolved in acetic acid (Molar), and lyophilized. The diastereomers were separated by using silica gel and semipreparative RP-HPLC with a Vydac 218TP1010 column as described in General Methods section. Purities were found to be over 98% as assessed by analytical RP-HPLC. The molecular weigths of the analogues were confirmed by mass spectrometry and are reported in Table S1 (see Supporting Information).

**Identification of Enantiomers of 2-Aminocyclopentanecarboxylic (ACPC) and 2-Aminocyclohexanecarboxylic (ACHC)**

**Acids in Peptides.** The configurations of the incorporated β-amino acids were determined after acidic hydrolysis of the peptides (6 M HCl, 24 h, 110 °C). The acidic hydrolyzates were separated by analytical RP-HPLC to isolate the β-amino acids. The absolute configurations of the purified alicyclic β-amino acids were determined by chiral TLC, and the $R_f$ values were then compared with those of optically pure alicyclic β-amino acid standards. GITC derivatization of the amino acid mixtures, followed by analytical HPLC analysis, was also used to confirm the configurations of the alicyclic β-amino acids. The retention times of the derivatized alicyclic β-amino acids were compared with those of the derivatized β-amino acid standards.[73]

**Rat Brain Membrane Preparation.** Rats (male, Wistar, 250−300 g) were caged in groups of four under a 12:12 h light/dark cycle, with free access to standard food and water until the time of sacrifice. The animals were handled according to the European Communities Council Directives (86/609/ECC) and the Hungarian Act for the Protection of Animals in Research (XXVIII. tv. Section 32). Crude membranes of rat forebrains were prepared as published elsewhere and kept frozen in liquid nitrogen.[39] Before the experiments, the brain homogenates were thawed, diluted with the working buffer and centrifuged at 20000*g* to remove sucrose. The pellet was homogenized with a Dounce in the appropriate volume of Tris-HCl buffer (50 mM, pH: 7.4). Protein content was determined by the method of Bradford, using BSA as a standard.[74]

**Radioligand Binding Assay.** Competition experimental conditions were optimized and varied, depending on the radioligand applied. The detailed description of the experimental setup has been published elsewhere.[34] Competition binding experiments were performed by incubating rat brain membranes (0.2−0.5 mg protein/tube) with 1 nM [$^3$H]DAMGO, 2 nM [$^3$H]Ile$^{5,6}$deltorphin-2 or 1 nM [$^3$H]endomorphin-2 and $10^{-10}$−$10^{-5}$ M unlabeled ligands. Nonspecific binding was determined with 10 μM naloxone and subtracted from the total binding to yield the specific binding. Radioactivity was measured in a toluene-based cocktail with a TRI-CARB 2100TR liquid scintillation counter (Canberra-Packard, Perkin-Elmer Life Sciences 549 Albany Street, Boston MA 02118). Results are reported as means ± SEM of the data of at least three independent measurements, each performed in duplicate. Inhibitory constants ($K_i$, nM) were calculated from the competition experiments by using nonlinear least-squares curve fitting and the Cheng−Prusoff equation,[75] with GraphPad Prism software (version 4.0, San Diego, CA).

**Ligand-Stimulated [$^{35}$S]GTPγS Functional Assay.** The detailed experimental procedure has been published elsewhere.[76] Briefly, rat forebrain membranes (10−15 μg protein/tube) were incubated with 0.05 nM [$^{35}$S]GTPγS and $10^{-10}$−$10^{-5}$ M unlabeled ligands in the presence of 30 μM GDP, 100 mM NaCl, 3 mM MgCl, and 1 mM EGTA in Tris-HCl buffer (50 mM, pH 7.4) for 60 min at 30 °C. Basal binding was measured in the absence of ligand and set at 100%. Nonspecific binding was determined with 10 μM unlabeled GTPγS and subtracted. The radioactivity of the filters was determined in a toluene-based cocktail with a TRI-CARB 2100TR liquid scintillation counter (Canberra-Packard, Perkin-Elmer Life Sciences). Data were expressed as the percentage stimulation of the specific [$^{35}$S]GTPγS binding over the basal activity and are given as means ± SEM Each measurement was performed in triplicate and analyzed with the sigmoidal dose−response curve fitting option of the GraphPad Prism software (version 4.0, San Diego, CA) to obtain potency ($ED_{50}$, the concentration of the ligand required to elicit the half-maximal effect) and efficacy ($E_{max}$, the maximal effect) values.

**NMR Spectroscopy.** Approximately 4 mg of compounds **2**, **3**, **11**, or **12** was dissolved in 0.5 mL DMSO-$d_6$ (Cambridge Isotopes). All NMR spectra were acquired at 300 K by using an inverse multinuclear (bbi) single-axis gradient 5 mm probe. Proton chemical shifts were referenced directly to the internal DMSO peak at 2.49 ppm. TOCSY and ROESY spectra were recorded in phase-sensitive mode with mixing times of 60 and 150 ms, respectively. TOCSY experiments were carried out with 4096 data points in $f_2$ and 512 data points in $f_1$, and 8 scans were collected at each increment. The MLEV-17 mixing sequence was flanked by simultaneously switched spin-lock and gradient pulses to obtain the signals of the pure absorption phase for coupling constant measurements. ROESY experiments were performed with 2048 data points in $f_2$ and 512 data points in $f_1$, and 64 scans were collected at each increment. Proton−proton scalar coupling constants were measured from the 1D $^1$H NMR and/or 2D TOCSY spectra, respectively. In the latter case, the corresponding rows extracted from the TOCSY spectra were inversely Fourier transformed and then zero-filled to 16 K real data points. A Gaussian function was applied prior to the Fourier transform and the final digital resolution of the resulting 1D traces was ca. 0.3 Hz. The coupling constants $^3J_{H\alpha-H\beta}$ were used to estimate the side chain rotamer populations along the $\chi_1$ angles in the Tyr, Phe, and Trp residues by using the Pachler equations with parameters appropriate for aromatic residues ($^{ap}J_{H\alpha-H\beta}$ = 13.9 Hz and $^{sc}J_{H\alpha-H\beta}$ = 3.55 Hz). The volumes of ROESY crosspeaks were converted into upper distance bounds, the intensities of the Tyr$^1$-$H_\beta$,$H_{\beta'}$ peaks being used for calibration.

**Computational Methods.** The TINKER 4.2 program package[77] was used for distance geometry calculations. One thousand structures were generated for each peptide with the inclusion of NOE-derived interproton distances as restraints. The peptide bond between Tyr$^1$ and ACPC$^2$ was kept in the *trans* configuration in all peptide analogues. The resultant structures were clustered to identify and eliminate duplicate structures from further analysis. Clustering was performed with the g_cluster utility of the GROMACS 3.3 program package[78] and the gromos[79] method with a 0.5 Å rmsd similarity cutoff, comparing positions of backbone atoms, amide hydrogens, amide carbonyl oxygens, and β-carbon atoms. Only the middle structures of the resultant clusters were subjected to further analysis. These geometries were energy-minimized by using the Amber 9 program package,[80] the generalized Amber force field (gAFF)[81] and the GB/SA implicit solvent model.[82] One thousand steps of steepest descent were followed by 1500 steps of conjugate gradient minimization where the convergence criteria for the energy gradient was $10^{-4}$ kcal mol$^{-1}$ Å and the long-range nonbonded interactions were calculated with a 10 Å cutoff. The resultant pool of structures was clustered again as described above to identify and eliminate structures corresponding to the same local energy minimum. The middle structures of these final clusters, which were regarded as possible geometries of the studied peptides, were analyzed one by one by using the VMD and the Molekel molecular visualization and analysis programs. For each peptide analogue, three dominant conformations were identified, which were then used as starting structures for MD simulations.

MD simulations were carried out with the Amber 9 program package and the gAFF force field parameter set. Each starting structure was immersed in a truncated octahedron box of TIP3P water molecules,[83] where each atom of the solute was no less than 8 Å from the edge of the water box. Solvent molecules were removed from the box when the distance between any atom of the solute molecule and any atom of the solvent molecule was less than the sum of the van der Waals radii of both atoms. Therefore, each starting structure was solvated with 749−1125 TIP3P water molecules. The charged N-termini of peptides were neutralized by replacing solvent molecules by chloride ions at the positions of the first solvent molecule with the most favorable electrostatic potential. All systems were then subjected to 500 steps of steepest descent followed by 500 steps of conjugate gradient energy minimization, all atoms of the solute molecule being fixed with a force constant 500 kcal mol$^{-1}$ Å$^2$. The position restraint was then removed and 1000 steps of steepest descent were followed by 1500 steps of conjugate gradient energy minimization on the whole system. Next, 100 ps NVT MD was performed with slow heating from 0 to 300 K and by positionally restraining the peptide in the center of the box with a force constant of 10 kcal mol$^{-1}$ Å$^2$ on each atom to allow the solvent density to equilibrate around the solute molecule. Then 50.25 ns NPT MD was performed for each system at constant temperature (300 K) and pressure (1 atm) with the following parameters: the time step was 2 fs, the SHAKE algorithm was utilized to constrain all bonds to their correct length, the Langevin thermal model with a collision frequency of 1.0 ps$^{-1}$ was applied to control the temperature, and the peptide and solvent were coupled to constant

pressure by using isotropic scaling with a relaxation constant of 2.0 ps. Nonbonded interactions were calculated via the PME method with a 10 Å cutoff. The coordinates of the peptide were stored after every 1000 steps to yield a total of 25000 sampled conformations for each trajectory after excluding the first 250 ps, which was regarded as the equilibration period. The trajectories resulting from the three different initial conformations were combined to yield a 150 ns long trajectory for each peptide.

The peptide structures of each trajectory were analyzed with the analysis programs of the GROMACS 3.3 program suite and Perl scripts written in-house. Clustering of structural ensembles was performed as described above, but with a 1 Å rmsd cutoff. Every tenth backbone coordinate set from the trajectories was included in the analysis, which resulted in 7500 × 7500 rmsd matrices. The structures along the trajectory were also probed for the existence of H-bonds by the g_h bond utility of GROMACS. The cutoff distance between a donor and an acceptor atom was set to 3.5 Å and 60° was taken as the cutoff for the donor−hydrogen−acceptor angle. The backbone structure was examined through measurement of the $N(1)-C_\alpha(2)-C_\alpha(3)-C(4)$ virtual dihedral angle and the distance between the terminal $C_\alpha$ atoms.[84] A bent structure was assigned when this dihedral angle was between −80° and 80° and the distance was less than 7 Å. The distances between the putative pharmacophore elements[40] and side chain rotamer populations were also determined.

**Acknowledgment.** This work was supported by OTKA grants TS 09817 (M.S., G.T.), NK 68578 (K.E.K., A.B.), and T 67563 (A.P.), an FP6 European grant (LSHC-CT-2006-037733) (G.T.), and an NKTH-DNT research grant 08/2004 (M.S., G.T.). The excellent technical assistance of Ildikó Németh and Éva Tóth is gratefully acknowledged

**Supporting Information Available:** Chromatograms of the purified peptide diastereomers; RP-HPLC, TLC, and MS data on all diastereomers and endomorphins; description and results of the stability experiment; $^1$H NMR chemical shifts (ppm) and coupling constants (*J* in Hz) for endomorphin-1 (**2** and **3**) and endomorphin-2 (**11** and **12**) analogues. Rotamer populations of the $Tyr^1$, $Phe^3$, or $Trp^3$, and $Phe^4$ side chains in endomorphin-1 (**2** and **3**) and endomorphin-2 (**11** and **12**) analogues. This material is available free of charge via the Internet at http://pubs.acs.org.

## References

(1) Janecka, A.; Fichna, J.; Janecki, T. Opioid receptors and their ligands. *Curr. Top. Med. Chem.* **2004**, *4*, 1–17.
(2) Wollemann, M.; Benyhe, S. Non-opioid action of opioid peptides. *Life Sci.* **2004**, *75*, 257–276.
(3) Zadina, J. E.; Hackler, L.; Ge, L. J.; Kastin, A. J. A potent and selective endogenous agonist for the mu-opiate receptor. *Nature* **1997**, *386*, 499–502.
(4) Hackler, L.; Zadina, J. E.; Ge, L. J.; Kastin, A. J. Isolation of relatively large amounts of endomorphin-1 and endomorphin-2 from human brain cortex. *Peptides* **1997**, *18*, 1635–1639.
(5) Martin-Schild, S.; Gerall, A. A.; Kastin, A. J.; Zadina, J. E. Differential distribution of endomorphin-1 and endomorphin-2-like immunoreactivities in the CNS of the rodent. *J. Comp. Neurol.* **1999**, *405*, 450–471.
(6) Spetea, M.; Monory, K.; Tömböly, Cs.; Tóth, G.; Tzavara, E.; Benyhe, S. In vitro binding and signaling profile of the novel $\mu$ opioid receptor agonist endomorphin 2 in rat brain membranes. *Biophys. Res. Commun.* **1998**, *250*, 720–725.
(7) Goldberg, I. E.; Rossi, G. C.; Letchworth, S. R.; Mathis, J. P.; Ryan-Moro, J.; Leventhal, L.; Su, W.; Emmel, D.; Bolan, E. A.; Pasternak, G. W. Pharmacological characterization of endomorphin-1 and endomorphin-2 in mouse brain. *J. Pharmacol. Exp. Ther.* **1998**, *286*, 1007–1013.
(8) Ronai, A. Z.; Szemenyei, E.; Kato, E.; Kocsis, L.; Orosz, G.; Al-Khrasani, M.; Toth, G. Endomorphin synthesis in rat brain from intracerebroventricularly injected [$^3$H]-Tyr-Pro: a possible biosynthetic route for endomorphins. *Regul. Pept.* **2006**, *134*, 54–60.
(9) Tömböly, Cs.; Péter, A.; Tóth, G. In vitro quantitative study of the degradation of endomorphins. *Peptides* **2002**, *23*, 1573–1580.
(10) Péter, A.; Tóth, G.; Tömböly, Cs.; Laus, G.; Tourwé, D. Liquid chromatographic study of the enzymatic degradation of endomorphins, with identification by electrospray ionization mass spectrometry. *J. Chromatogr.* **1999**, *846*, 39–48.
(11) Kastin, A. J.; Fasold, M. B.; Smith, R. R.; Horner, K. A.; Zadina, J. E. Saturable brain-to-blood transport of endomorphins. *Exp. Brain. Res.* **2001**, *139*, 70–75.
(12) Koda, Y.; Shiotani, K.; Toth, I.; Tsuda, Y.; Okada, Y.; Blanchfield, Y. T. Comparison of the in vitro apparent permeability and stability of opioid mimetic compounds with that of the native peptide. *Bioorg. Med. Chem. Lett.* **2007**, *17*, 2043–2046.
(13) Horvath, Gy.; Szikszay, M.; Tomboly, C.; Benedek, G. Antinociceptive effects of intrathecal endomorphin-1 and−2 in rats. *Life Sci.* **1999**, *65*, 2635–2641.
(14) Obara, I.; Przewlocki, R.; Przewlocka, B. Local peripheral effects of $\mu$-opioid receptor agonists in neurophatic pain in rats. *Neurosci. Lett.* **2004**, *360*, 85–89.
(15) Przewlocka, B.; Mika, J.; Labuz, D.; Toth, G.; Przewlocki, R. Spinal analgesic action of endomorphins in acute, inflammatory and neuropathic pain in rats. *Eur. J. Pharmacol.* **1999**, *367*, 189–196.
(16) Czapla, M. A.; Gozal, D.; Alea, O. A.; Beckerman, R. C.; Zadina, J. E. Differential Cardiorespiratory Effects of Endomorphin-1, Endomorphin-2, DAMGO, and Morphine. *Am. J. Respir. Crit. Care. Med.* **2000**, *162*, 994–999.
(17) Gentilucci, L.; Tolomelli, A. Recent Advances in the Investigation of the Bioactive Conformation of Peptides Active at the $\mu$-opioid Receptor. Conformational Analysis of Endomorphins. *Curr. Top. Med. Chem.* **2004**, *4*, 105–121.
(18) Janecka, A.; Staniszewska, R.; Fichna, J. Endomorphin Analogs. *Curr. Med. Chem.* **2007**, *14*, 3201–3208.
(19) Podlogar, B. L.; Paterlini, M. G.; Ferguson, D. M.; Leo, G. C.; Demeter, D. A.; Brown, F. K.; Reitz, A. B. Conformational analysis of the endogenous $\mu$-opioid agonist endomorphin-1 using NMR spectroscopy and molecular modeling. *FEBS Lett.* **1998**, *439*, 13–20.
(20) Fiori, S.; Renner, C.; Cramer, J.; Pegoraro, S.; Moroder, L. Preferred conformation of endomorphin-1 in aqueous and membrane mimetic environments. *J. Mol. Biol.* **1999**, *291*, 163–175.
(21) Paterlini, M. G.; Avitabile, F.; Ostrowski, B. G.; Ferguson, D. M.; Porthogese, P. S. Stereochemical requirements for receptor recognition of the $\mu$-opioid peptide endomorphin-1. *Biophys. J.* **2000**, *78*, 590–599.
(22) Tomboly, C.; Kover, K. E.; Peter, A.; Tourwe, D.; Biyashev, D.; Benyhe, S.; Borsodi, A.; Al-Khrasani, M.; Ronai, A. Z.; Toth, G. Structure−activity study on the Phe side chain arrangement of endomorphins using conformationally constrained analogues. *J. Med. Chem.* **2004**, *47*, 735–743.
(23) Li, T.; Jinsmaa, Y.; Nedachi, M. M. A.; Tsuda, Y.; Ambo, A.; Sasaki, Y.; Bryant, S. D.; Marczak, E.; Li, Q.; Swartzwelder, H. S.; Lazarus, L. H.; Okada, Y. Transformation of mu-opioid receptor agonists into biologically potent mu-opioid receptor antagonist. *Bioorg. Med. Chem.* **2007**, *15*, 1237–1251.
(24) Fichna, J.;do-Rego, J. C.;Janecka, T.;Staniszewska, R.;Poels, J.;Broeck, J. V.;Costentin, J.;Schiller, P. W.;Janecka, A. Novel highly potent mu-opioid receptor antagonist based on endomorphin-2 structure. *Bioorg. Med. Chem.* **2008**, (Epub ahead of print).
(25) Sasaki, Y.; Sasaki, A.; Niizuma, H.; Goto, H.; Ambo, A. Endomorphin 2 Analogues Containing Dmp Residue as an Aromatic Amino Acid Surrogate with High $\mu$-Opioid Receptor Affinity and Selectivity. *Bioorg. Med. Chem.* **2003**, *11*, 675–678.
(26) Leitgeb, B. Structural Investigation of Endomorphins by Experimental and Theoretical Methods: Hunting for the Bioactive Conformation. *Chem. Biodiversity* **2007**, *4*, 2703–2724.
(27) In, Y.; Minoura, K.; Ohishi, H.; Minakata, H.; Kamigauchi, M.; Sugiura, M.; Ishida, T. Conformational comparison of m-selective endomorphin-2 with its C-terminal free acid in DMSO solution, by $^1$H NMR spectroscopy and molecular modeling calculation. *J. Pept. Res.* **2001**, *58*, 399–412.
(28) Cardillo, G.; Gentilucci, L.; Melchiorre, P.; Spampinato, S. Synthesis and binding activity of endomorphin-1 analogues containing $\beta$-amino acids. *Bioorg. Med. Chem. Lett.* **2000**, *10*, 2755–2758.
(29) Cardillo, G.; Gentilucci, L.; Qasem, A. R.; Sgarzi, F.; Spampinato, S. Endomorphin-1 analogues containing $\beta$-proline are mu-opioid receptor agonists and display enhanced enzymatic hydrolysis resistance. *J. Med. Chem.* **2002**, *45*, 2571–2578.
(30) Fülöp, F. The Chemistry of 2-Aminocycloalkanecarboxylic Acids. *Chem. Rev.* **2001**, *101*, 2181–2204.
(31) Fülöp, F.; Martinek, T. A.; Tóth, K. G. Application of alicyclic $\beta$-amino acids in peptide chemistry. *Chem. Soc. Rev.* **2006**, *35*, 323–334.
(32) Steer, L. D.; Lew, A. R.; Perlmutter, P.; Smith, I. A.; Aguilar, I. M. $\beta$-Amino Acids: Versatile Peptidomimetics. *Curr. Med. Chem.* **2002**, *9*, 811–822.
(33) Kuhl, A.; Hahn, M. G.; Dumic, M.; Mittendorf, J. Alicyclic $\beta$-amino acids in Medicinal Chemistry. *Amino Acids* **2005**, *29*, 89–100.
(34) Bozó, B.; Fülöp, F.; Tóth, K. G.; Tóth, G.; Szűcs, M. Synthesis and opioid binding activity of dermorphin analogues containing cyclic $\beta$-amino acids. *Neuropeptides* **1997**, *31*, 367–372.

(35) Yamazaki, T.; Pröbstl, A.; Schiller, P. W.; Goodman, M. Biological and conformational studies of [Val[4]]morphiceptin and [D-Val[4]]morphiceptin analogs incorporating *cis*-2-aminocyclopentane carboxylic acid as a peptidomimetic for proline. *Int. J. Peptide Protein Res* **1991**, *37*, 364–381.

(36) Mierke, D. F.; Nöbner, G.; Schiller, P. W.; Goodman, M. Morphiceptin analogs containing 2-aminocyclopentane carboxylic acid as a peptidomimetic for proline. *Int. J. Pept. Protein Res.* **1990**, *35*, 35–45.

(37) Tóth, G.; Fülöp, F.; Péter, A.; Fábián, G.; Murányi, M.; Horváth, Gy.; Szűcs, M. New endomorphin analogues using β-amino acids as proline mimetics in position 2. *Proceedings of the 27th European Peptide Symposium*; Benedetti, E., Pedone, C., Eds.; Edizioni Ziino: Napoli, Italy, 2002; pp 630−631.

(38) Tóth, G.; Keresztes, A.; Tömböly, Cs.; Péter, A.; Fülöp, F.; Tourwé, D.; Navratilova, E.; Varga, É; Roeske, W. R.; Yamamura, H. I.; Szűcs, M.; Borsodi, A. New endomorphin analogs with μ-agonist and δ-antagonist properties. *Pure Appl. Chem.* **2004**, *76*, 951–957.

(39) Keresztes, A.; Tóth, G.; Fülöp, F.; and Szűcs, M. Synthesis, radiolabeling and receptor binding of [$^3$H][(1S,2R)ACPC$^2$]endomorphin-2. *Peptides* **2006**, *27*, 3315–3321.

(40) Yamazaki, T.; Ro, S.; Goodman, M.; Chung, N. N.; Schiller, P. W. A topochemical approach to explain morphiceptin bioactivity. *J. Med. Chem.* **1993**, *36*, 708–719.

(41) Schiller, P. W.; Weltrowska, G.; Berezowska, I.; Nguyen, T. M.; Wilkes, B. C.; Lemieux, C.; Chung, N. N. The TIPP opioid peptide family: development of delta antagonists, delta agonists, and mixed mu agonist/delta antagonists. *Biopolymers (Pept. Sci.)* **1999**, *51*, 411–425.

(42) Rónai, A. Z.; Al-Khrasani, M.; Benyhe, S.; Lengyel, I.; Kocsis, L.; Orosz, G.; Tóth, G.; Kató, E.; Tóthfalusi, E. Partial and full agonism in endomorphin derivatives: comparison by null and operational model. *Peptides* **2006**, *27*, 1507–1513.

(43) Sim, L. J.; Liu, Q.; Childers, S. R.; Selley, D. E. Endomorphin-stimulated [$^{35}$S]GTPγS binding in rat brain: evidence for partial agonist activity at mu opioid receptor. *J. Neurochem.* **1998**, *70*, 1567–1576.

(44) Temussi, P. A.; Picone, D.; Saviano, G.; Amodeo, G.; Motta, A.; Tancredi, T.; Salvadori, S.; Tomatis, R. Conformational analysis of an opioid peptide in solvent media that mimic cytoplasm viscosity. *Biopolymers* **1992**, *32*, 367–372.

(45) Jackson, M.; Mantsch, H. H. Beware of protein in DMSO. *Biochim. Biophys. Acta* **1991**, *1078*, 231–235.

(46) Wüthrich, K. *NMR of Proteins and Nucleic Acids*; Wiley: New York, 1986.

(47) Kövér, K. E.; Uhrin, D.; Hruby, V. J. Gradient- and Sensitivity-Enhanced TOCSY Experiments. *J. Magn. Reson.* **1998**, *130*, 162–168.

(48) Pachler, K. G. R. Nuclear Magnetic Resonance Study of Some Alpha-Amino Acids. 1. Coupling Constants in Alkaline and Acidic Medium. *Spectrochimica* **1963**, *19*, 2085–2092.

(49) Pachler, K. G. R. Nuclear Magnetic Resonance Study of Some Alpha-Amino Acids. 2. Rotational isomerism. *Spectrochim. Acta* **1964**, *20*, 581–587.

(50) Kabsch, W.; Sander, C. Dictionary of protein secondary structure: Pattern recognition of hydrogen-bonded and geometrical features. *Biopolymers* **1983**, *22*, 2577–2637.

(51) Frishman, D.; Argos, P. Knowledge-based protein secondary structure assignment. *Proteins* **1995**, *23*, 566–579.

(52) Ide, S.; Sakano, K.; Seki, T.; Awamura, S.; Minami, M.; Satoh, M. Endomorphin-1 discriminates the mu-opioid receptor from the delta- and kappa-opioid receptors by recognizing the difference in multiple regions. *Jpn. J. Pharmacol.* **2002**, *83*, 306–311.

(53) Seki, T.; Minami, M.; Nakagawa, T.; Ienaga, Y.; Morisada, A.; Satoh, M. DAMGO recognizes four residues in the third extracellular loop to discriminate between mu- and kappa-opioid receptors. *Eur. J. Pharmacol.* **1998**, *350*, 301–310.

(54) Wu, H. E.; Hung, K. C.; Mizoguchi, H.; Fujimoto, J. M.; Tseng, L. F. Acute antinociceptive tolerance and asymmetric cross-tolerance between endomorphin-1 and endomorphin-2 given intracerebroventricularly in the mouse. *J. Pharmacol. Exp. Ther.* **2001**, *299*, 1120–1125.

(55) Tseng, L. F. The antinociceptive properties of endomorphin-1 and endomorphin-2 in the mouse. *Jpn. J. Pharmacol.* **2002**, *89*, 216–220.

(56) Venkatesan, P.; Baxi, S.; Evans, C.; Neff, R.; Wang, X.; Mendelowitz, D. Glycinergic inputs to cardiac vagal neurons in the nucleus ambiguus are inhibited by nociceptin and mu-selective opioids. *J. Neurophysiol.* **2003**, *90*, 1581–1588.

(57) Snook, L. A.; Milligan, G.; Kieffer, B. L.; Massotte, D. μ-δ Opioid Receptor Functional Interaction: Insight Using Receptor-G Protein Fusions. *J. Pharmacol. Exp. Ther.* **2006**, *318*, 683–690.

(58) Gomes, I.; Gupta, A.; Filipovska, J.; Szeto, H. H.; Pintar, J. E.; Devi, L. A. A role for heterodimerization of μ and δ opiate receptors in enhancing morphine analgesia. *Proc. Natl. Acad. Sci. U.S.A.* **2004**, *101*, 5135–5139.

(59) George, S. R.; Fan, T.; Xie, Z.; Tse, R.; Tam, V.; Varghese, G.; O′ Dowd, B. F. Oligomerization of μ- and δ-opioid receptors. Generation of novel functional properties. *J. Biol. Chem.* **2000**, *275*, 26128–26135.

(60) Gomes, I.; Jordan, B. A.; Gupta, A.; Trapaidze, N.; Nagy, V.; Devi, L. A. Heterodimerization of μ and δ opioid receptors: a role in opiate synergy. *J. Neurosci.* **2000**, *20*, RC110.

(61) Ho, M.; Wong, Y. H. $G_z$ signaling: emerging divergence from $G_i$ signaling. *Oncogene* **2001**, *20*, 1615–1625.

(62) Martin, N. A.; Prather, P. L. Interaction of co-expressed μ- and δ-opioid receptors in transfected rat pituitary $GH_3$ cells. *Mol. Pharmacol.* **2001**, *59*, 774–783.

(63) Jardetzky, O. On the nature of molecular conformations inferred from high-resolution NMR. *Biochim. Biophys. Acta* **1980**, *621*, 227–232.

(64) Eguchi, M.; Shen, R. Y. W.; Shea, J. P.; Lee, M. S.; Kahn, M. Design, Synthesis and Evaluation of Opioid Analogues with Non-Peptidic β-Turn Scaffold: Enkephalin and Endomorphin Mimetics. *J. Med. Chem.* **2002**, *45*, 1935–1938.

(65) Leitgeb, B.; Ötvös, F.; Tóth, G. Conformational Analysis of Endomorphin-2 by Molecular Dynamics Methods. *Biopolymers* **2002**, *68*, 497–511.

(66) Ötvös, F.; Körtvélyesi, T.; and Tóth, G. Structure−activity relationships of endomorphin-1, endomorphin-2 and morphiceptin by molecular dynamics methods. *J. Mol. Struct. (THEOCHEM)* **2003**, *666−667*, 345–353.

(67) Yao, J.; Feher, V. A.; Espejo, B. F.; Reymond, M. T.; Wright, P. E.; Dyson, H. J. Stabilization of a type VI turn in a family of linear peptides in water solution. *J. Mol. Biol.* **1994**, *243*, 736–753.

(68) Yao, J.; Dyson, H. J.; Wright, P. E. Three dimensional structure of a type VI turn in a linear peptide in water solution. Evidence for stacking of aromatic rings as a major stabilizing factor. *J. Mol. Biol.* **1994**, *243*, 754–766.

(69) Forró, E.; Fülöp, F. Advanced procedure for the enzymatic ring opening of unsaturated alicyclic β-lactams. *Tetrahedron: Asymmetry* **2004**, *15*, 2875–2880.

(70) Forró, E.; Fülöp, F. Lipase-Catalyzed Enantioselective Ring Opening of Unactivated Alicyclic-Fused β-Lactams in an Organic Solvent. *Org. Lett.* **2003**, *5*, 1209–1212.

(71) Forró, E.; Fülöp, F. The first direct enzymatic hydrolysis of alicyclic β-amino esters, - a route to enantionpure cis and trans β-amino acids. *Chem.−Eur. J.* **2007**, *22*, 6397–6401.

(72) Kaiser, E.; Colescott, R. L.; Bossinger, C. D.; Cook, P. I. Color test for detection of free terminal amino groups in the solid-phase synthesis of peptides. *Anal. Biochem.* **1970**, *34*, 595–598.

(73) Péter, A.; Fülöp, F. High performance liquid chromatographic methods for the separation of isomers of *cis*- and *trans*-2-aminocyclopentane carboxylic acid. *J. Chromatogr., A* **1995**, *715*, 219–226.

(74) Bradford, M. M. A rapid and sensitive method for quantitation of microgram quantities of protein utilizing the principle of protein−dye binding. *Anal. Biochem.* **1976**, *72*, 248–254.

(75) Cheng, Y.; Prusoff, W. H. Relationship between the inhibition constant ($K_I$) and the concentration of inhibitor which causes 50% inhibition ($I_{50}$) of an enzymatic reaction. *Biochem. Pharmacol.* **1973**, *22*, 3099–3108.

(76) Fábián, G.; Bozó, B.; Szikszay, M.; Horváth, G.; Coscia, C. J.; Szűcs, M. Chronic morphine-induced changes in mu-opioid receptors and G proteins of different subcellular loci in rat brain. *J. Pharmacol. Exp. Ther.* **2002**, *302*, 774–780.

(77) *TINKER*, 2008. The TINKER software package is available free at http://dasher.wustl.edu/tinker/.

(78) Van der Spoel, D.; Lindahl, E.; Hess, B.; van Buuren, A. R.; Apol, E.; Meulenhoff, P. J.; Tieleman, D. P.; Sijbers, A.L.T.M.; Feenstra, K. A.; van Drunen, R.; Berendsen, H. J. C. *Gromacs User Manual, version 3.3*, 2005; www.gromacs.org.

(79) Daura, X.; Gademann, K.; Jaun, B.; Seebach, D.; van Gunsteren, W. F.; Mark, A. E. Peptide Folding: When Simulation Meets Experiment. *Angew. Chem., Int. Ed.* **1999**, *38*, 236–240.

(80) Case, D. A.; Daren T. A.; Cheatham, T. E. I.; Simmerling, C. L.; Wang, J.; Duke, R. E.; Luo, R.; Merz, K. M.; Pearlman, D. A.; Crowley, M.; Walker, R. C.; Zhang, W.; Wang, B.; Hayik, S.; Roitberg, A.; Seabra, G.; Wong K. F.; Paesani, F.; Wu, X.; Brozell, S.; Tsui, V.; Gohlke, H.; Yang, L.; Tan, C.; Mongan, L.; Hornak, V.; Cui, G.; Beroza, P.; Matthews, D. H.; Schafmeister, C.; Ross, W. S.; Kollman, P. A. *AMBER 9*; University of California: San Francisco, 2006.

(81) Wang, J.; Wolf, R. M.; Caldwell, J. W.; Kollman, P. A. Development and testing of a general Amber force field. *J. Comput. Chem.* **2004**, *25*, 1157–1174.

(82) Still, W. C.; Tempczyk, A.; Hawley, R. C.; Hendrickson, T. Semianalytical treatment of solvation for molecular mechanics and dynamics. *J. Am. Chem. Soc.* **1990**, *112*, 6127–6129.

(83) Jorgensen, W. L.; Chandrasekhar, J.; Madura, J.; Klein, M. L. Comparison of Simple Potential Functions for Simulating Liquid Water. *J. Chem. Phys.* **1983**, *79*, 926–935.

(84) Ball, J. B.; Hughes, R. A.; Alewood, P. F.; Andrews, P. R. β-Turn topography. *Tetrahedron* **1993**, *49*, 3467–3478.

JM800223T